

Warith Scientific Journal of Engineering and Technology

Journal homepage: wsjet.uowa.edu.iq

Improving Formability of Low-Carbon Steel Shells through Deep Drawing: Experimental Analysis using SPSS

Yousif Sabah Kareem

Islamic Azad University, Science and Research Branch, Tehran, Faculty of Mechanical, Electrical and Computer Engineering

*Corresponding author E-mail address: yousif.iq1985@gmail.com

ARTICLEINFO

Keywords: sheet metal forming deep drawing bootstrapping formability SPSS analysis

ABSTRACT

Deep drawing, a prevalent sheet metal forming technique, is beset by fracture, wrinkling, and earing. This research investigates punch velocity, die curvature, and lubrication to enhance the formability of low-carbon steel cups. These parameters were selected due to their direct influence on forming force, metal flow, and thickness distribution, which dictate product quality. This study examines the impact of speed, radius, and lubrication on formability. The pressure of the blank holder and the height of the die can also influence formability. Experiments designed by DOE approach were assessed using SPSS and validated by Bootstrapping. Speed was the primary element influencing forming force and thickness; however, die radius and lubrication had a greater impact on force. Utilizing lubrication (oil or grease) at a rate of 200 mm/min with a die radius of 6-8 mm diminished thinning and friction relative to dry conditions, producing optimal outcomes. The regression models demonstrated R2 values of 64.3% for force and 78.7% for thickness, so confirming their validity. A thorough experimental validation demonstrates that in typical deep drawing of low-carbon steel, speed is the predominant factor, while lubrication enhances surface quality. This research enhances traditional deep drawing through statistically validated models, offering novel guidelines to augment manufacturing efficiency and product reliability. Prior research concentrated on blank-holder pressure or sophisticated shaping methodologies.

1 Introduction

Sheet metal forming, especially deep drawing, is an essential method for manufacturing lightweight structural components with intricate geometries in sectors such as automotive and appliances. Notwithstanding its prevalent application, traditional deep drawing frequently encounters significant drawbacks such as fracture, wrinkling, thinning, and earing, which compromise the precision and dependability of the final output. The ongoing faults highlight the research issue: how to systematically enhance the formability of low-carbon steel shells while preserving process simplicity and cost-effectiveness [1]. Previous research has investigated many factors affecting formability. Investigations investigating blank-holder pressure and beginning fluid pressure demonstrated substantial effects on strain distribution and limiting drawing ratios, while other studies examined the impact of punch shape, material composition, and extreme temperatures. While significant, much of this research pertains to specific or advanced forming techniques. The combined influence of conventional parameters—specifically punch speed, die radius, and lubrication—remains

https://doi.org/10.57026/wsjet.v1i1.21

inadequately examined, particularly through the application of rigorous statistical methods to determine their individual and interactive effects on product quality [2, 3].

This study purposefully selected these factors as they dictate the most crucial outcomes: forming force, thickness distribution, and surface quality. To eradicate ambiguity in **Figure 1**, the symbols are elucidated: Rp represents the punch radius, Rd signifies the die profile radius, t0 indicates the beginning sheet thickness, and V defines the punch speed [4, 5].

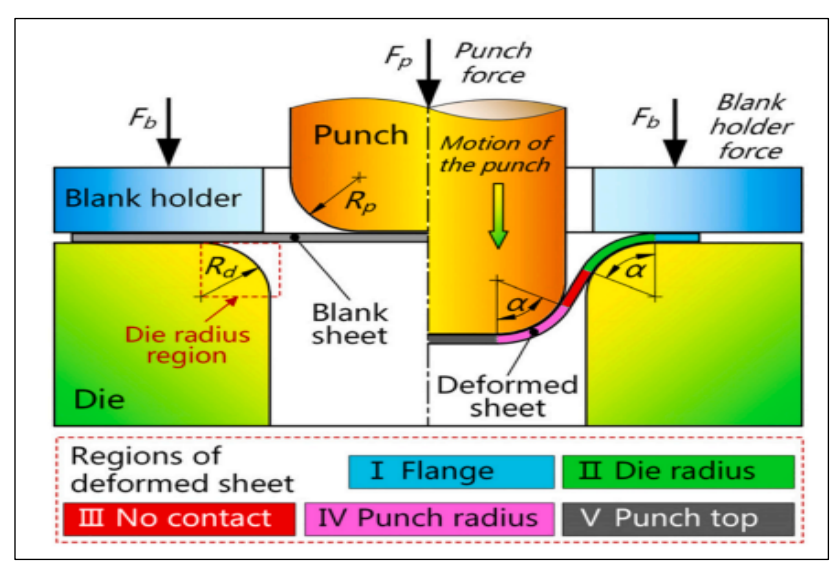


Figure 1. A schematic of cup deep drawing process [5]

Numerous studies concentrate on the impact of process factors on formability. Tommerup et al. investigated the effect of blank holder pressure (BHP) on strain trajectories in sheet metal forming. They created a specific tooling system that can modify BHP across eight unique configurations, allowing for precise regulation of material flow. This system integrated a controller for parameter regulation, an actuator for BHP management, and a tool embedded with hydraulic cavities. Strain routes were validated by modifying cavity pressures. The research entailed the creation of rectangular specimens [6].

In a separate study [7], Van Tung Phan conducted numerical simulations of the deep drawing process for ferritic stainless steel, examining the impact of variations in blank-holder pressure and friction on the earing profile. The simulated results were validated by empirical evidence.

To enhance the quality and stability of the deep drawing process for square cups made from a low-carbon steel alloy [8] the researcher investigated the relationship between forming pressure and input parameters, including blank holder force, frictional conditions, and die height.

An independent experimental investigation [9] examined the influence of several HDD process parameters on the draw ability of distinct metals. The researchers created a test apparatus capable of producing both symmetric and asymmetric cups. They noted that wrinkling was more pronounced in hydroforming compared to ordinary deep drawing. Failures in cup formation were alleviated by modifying the initial fluid pressure. The maximum forming pressures ranged from 0.15 to 0.3 times the average flow stress of the material. The limiting drawing ratio (LDR) was determined by the largest diameter of the blank that could be effectively created. Elevated strain hardening coefficients led to enhanced LDR values in HDD relative to traditional approaches, attributable to more uniform material deformation. The research also validated that the initial internal pressure substantially influences the hydroforming process results.

Sokolovan investigated the formability of layered composite sheets, highlighting the influence of punch shape and core thickness on sandwich systems. As the thickness of the polymer core increased from 0.2 mm to 1.0 mm, the necessary drawing force diminished. Nevertheless, the augmentation of the polymer cores resulted in an enhanced radius of the inner metallic shell, consequently diminishing deformation. Although augmented core thickness enhanced drawing by diminishing resistance, excessive thickness (0.2–1.6 mm) resulted in cracking in the cup head and edge areas during the application of a circular punch. Significantly, specimens possessing a 2.0 mm core thickness did not demonstrate such failures. Flange wrinkling was seen in all configurations, irrespective of thickness [10].

Jayahari and colleagues investigated the degree to which austenitic stainless steel may be formed when subjected to high temperatures. Their studies indicated that the LDR might attain a value of 2.5 at temperatures reaching 300 °C. Elevated temperatures reduced friction and residual strains, therefore improving product quality. Aluminum alloys exhibited enhanced draw ability under these conditions [11].

The work in [12] presented the restricted formability of AISI 1006 low-carbon steel in traditional deep drawing processes. The researchers created an innovative sheet hydroforming apparatus and demonstrated that this technique attained complete die depth with little thinning and enhanced corner quality. Conversely, conventional deep drawing attained merely 70% of the complete die depth owing to significant thinning and localized distortion.

Hwang et. al [13] examine the process analysis and pass design of compound deep drawing combined with ironing processes for A7075 aluminum alloy. Finally, Rao et.al [14] examine advanced deep drawing methods, associated challenges, and future prospects.

This research integrates experimental analysis with contemporary statistical methodologies, in contrast to previous efforts that frequently focus on individual case studies. The Design of Experiments (DOE) methodology guarantees systematic change of parameters, while SPSS analysis and Bootstrapping improve result validity despite restricted sample sizes. Recent developments in statistical modeling for metal forming [1, 2, 14] underscore the increasing significance of incorporating DOE/SPSS into manufacturing research. This study fills the gap by empirically and statistically assessing speed, radius, and lubrication in low-carbon steel deep drawing, with the objective of providing optimum parameter ranges and verified models to enhance formability in conventional procedures.

2 Methods of Experiments

<=0.08

The

Content Test

AISI

2.1 The Chemical Composition of Sheet Material

>=0.04

0.25 - 0.4

Steel is widely utilized, especially plain carbon steel. Low carbon steel (LCS) is a common plain carbon steel with low carbon content. It is the most common steel used in sheet metal work for car parts and appliances. The work-piece material in this investigation was 0.5 mm thick low-carbon steel due of its formability, price, and availability. **Table 1** presents the chemical composition of the AISI 1006 steel alloy examined in the study. The State Company for Inspection and Engineering Rehabilitation (S.I.E.R) evaluated the chemical composition in accordance with ASTM E415 criteria.

Table 1: (1006) AISI to Chemical Composition Content in [wt%] C% Mn% P% S%Cr% Ni% Mo% Al% 0.0636 0.0755 0.195 0.016 0.0060.0177 < 0.005 < 0.004 < 0.002

<=0.05

Thus, twenty-seven circular specimens were made using water jet machining (model no. 3020, Yonoda, China) as seen in **Figure 2**.

 $\leq = 0.04$

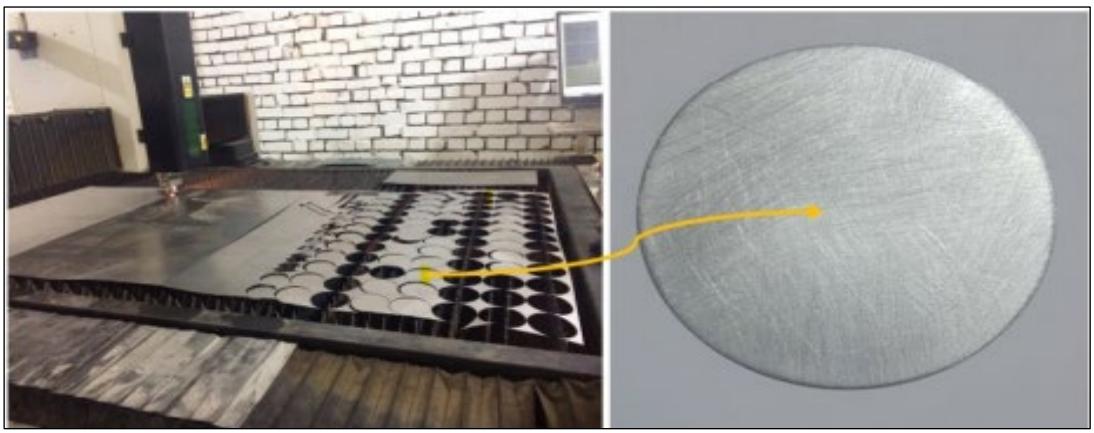


Figure 2. Initial Blank Process Preparation

2.2 The Mechanical properties of AISI 1006 low-carbon steel

The mechanical qualities of low-carbon steel (AISI 1006) are crucial to elucidate its selection for this investigation, alongside its chemical composition. Low-carbon steel alloys are distinguished by their excellent formability, favorable ductility, and cost-effectiveness relative to other alloys, rendering them especially appropriate for deep drawing processes. **Table 2** enumerates the principal mechanical parameters of the utilized alloys, encompassing yield strength, tensile strength, elongation, and hardness, in accordance with ASTM standards. These properties establish a fundamental framework for comprehending the metal's behavior during tests and facilitate the interpretation of results concerning formability and the quality of the final product [15].

Table 2. Mechanical properties of AISI 1006 low-carbon steel

Property	Value	Standard Reference		
Yield Strength (MPa)	170 - 210	ASTM E8/E8M		
Tensile Strength (MPa)	290 - 370	ASTM E8/E8M		
Elongation (%)	30 - 40	ASTM E8/E8M		
Hardness (HB)	90 - 110	ASTM E10		

2.3 Preparing for an experiment

In this study, a punch and die were created and constructed to manufacture round cups, as illustrated in Figure 3, which depicts a schematic illustration of the deep drawing tooling rig. They are fabricated from tool steel and have been machined. The stiff circle punch measures 80 mm and has utilized three dies. The radii of each component (4 mm, 6 mm, and 8 mm) and the punch corner radius is 5 mm, resulting in a radial clearance of 1.1 mm during assembly. Experiments in deep drawing are conducted to produce round cups, utilizing a deep drawing die attached to a Universal testing machine, model WDW-200E, which has a capacity of 200 kN. As the blank rests on the blank holder surface, the die moves downward towards the punch, indicating the application of an inverted drawing die. Three drawing speeds of 1, 100, and 200 mm/min were chosen for the low-carbon steel material. The blank holding force was established through trial and error as the least required to prevent wrinkling, which was proven to be 15 kN for low carbon steel material. A grid pattern of circles with radii of 5, 10, 15, 20, 25, 30, 35, etc., was produced using laser printing as shown in Figure 4 (a, b), to facility the measure of thickness along the cup wall. Some of products have been produced in this study present in Figure 4 (c, d); A digital thickness micrometer was employed to ascertain the wall thickness of the drawn cup. The micrometer featured a resolution of 0.001 mm and an accuracy tolerance of ± 0.003 mm, rendering it appropriate for the exact measurements necessary in formability research, as depicted in Figure 5. The number of 27 experiments was derived from a 3³ full factorial DOE design, with three levels of each factor (speed, die radius, lubrication). This ensures sufficient coverage of parameter combinations and allows the effects and interactions to be statistically validated. And to minimize measurement errors, we undertook the following actions

- Each specimen's thickness was measured at multiple grid points (5 mm intervals).
- The micrometer was calibrated before use and handled under constant pressure to avoid deformation.
- Repeated measurements were averaged, reducing random error.
- Environmental factors (temperature, vibration) were controlled during testing.

3 Experimental results

Lubrication is essential in the hydraulic sheet forming process utilizing a die, profoundly influencing the metal flow across the die surface, particularly during the drawing phase. Upon contact between the sheet metal and the die, frictional forces emerge between the two surfaces. These forces obstruct the metal's motion and can produce diverse consequences on the forming process. To analyze the impact of friction in the punch and die process, two situations were experimentally examined: the dry state and the lubricated state. No lubrication is supplied between the forming die and the sheet material surfaces in the dry state.

In the lubricated condition, two scenarios were examined: the first entails the application of a thin layer of grease to the low-carbon steel sheet, while the second involves the application of a thin film of oil between the sheet flange and the die surfaces.

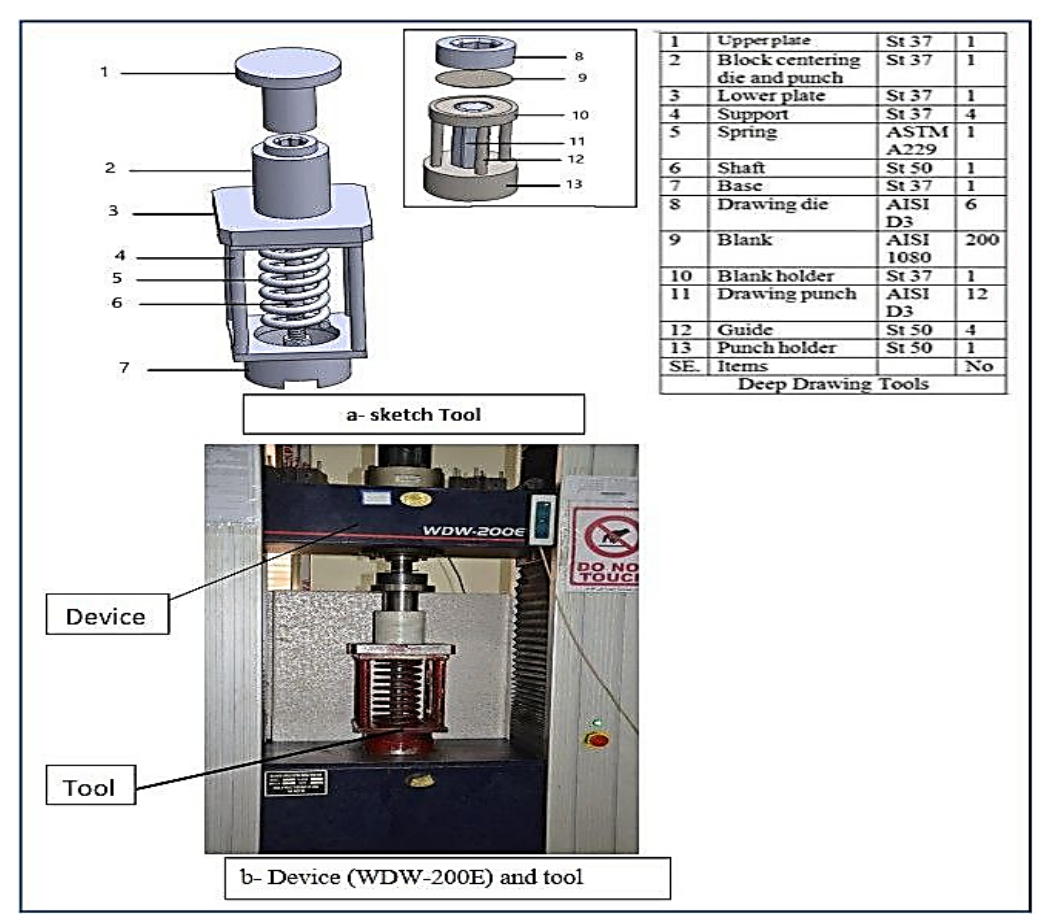


Figure 3. Experimental Configuration Utilized in this study: (a) Actual Image, (b) Schematic Representation

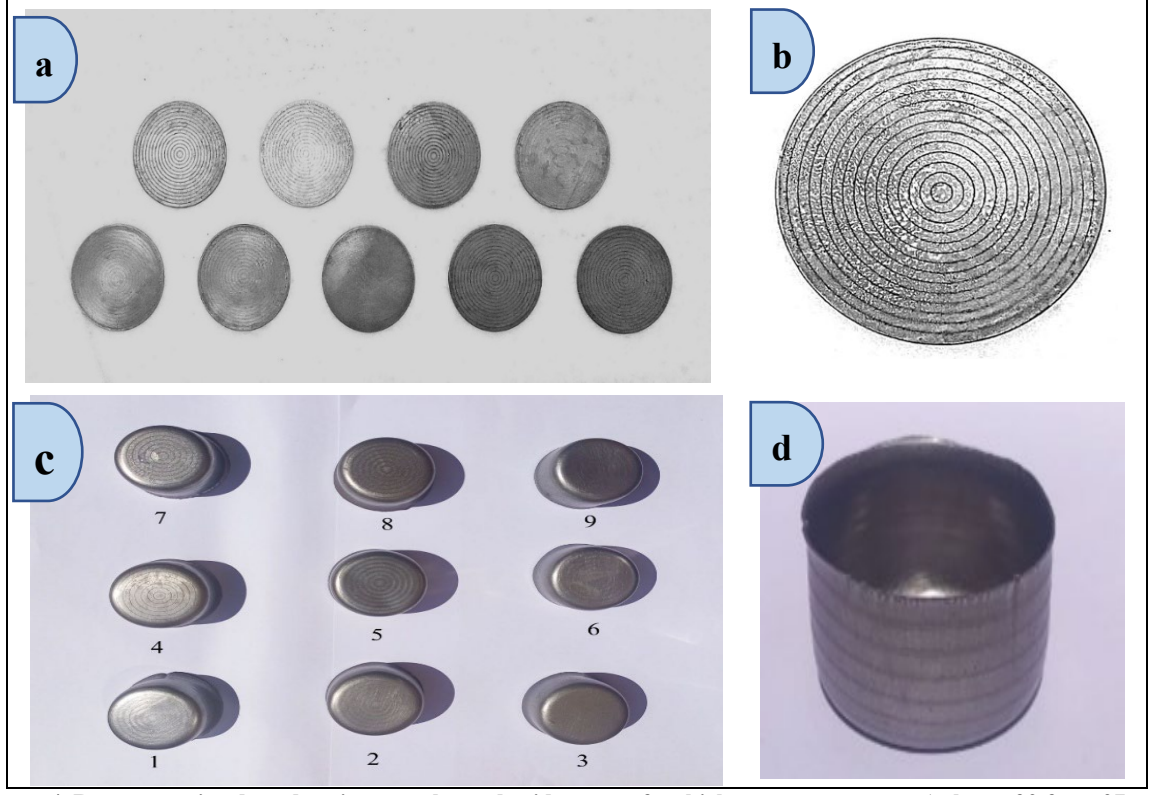


Figure 4. Representative deep drawing samples and grid pattern for thickness measurement (subset of 9 from 27 total experiments)



Figure 5. Digital Thickness Micrometer

The process parameter values were determined based on prior research, while maintaining other geometric parameters constant. **Table 3** presents the input parameters (speed, die profile radius, lubrication) with three levels (low, medium, high) and outputs (maximum force, lowest thickness).

Table 3: The Experimental samples

No. of Exp. Units of variables	X1 (Speed) mm/min	X2 (Radius) mm	X3 (Lubrication) without Lub. =0.42, With Lub. (Oil=0.081, Grease=0.078)	Y1 (Max Force) kN	Y2 (Low thickness) mm
1	1	8	0.081	21.64	0.4149
2	1	4	0.42	22.70	0.4151
3	1	6	0.078	21.80	0.4155
4	1	6	0.42	22.70	0.4158
5	1	8	0.42	22.64	0.4200
6	1	4	0.081	22.66	0.4171
7	1	6	0.081	21.81	0.4155
8	1	4	0.078	22.66	0.4171
9	1	8	0.078	21.64	0.4149
10	100	4	0.081	22.75	0.4207
11	100	8	0.078	22.08	0.4184
12	100	6	0.42	22.74	0.4182
13	100	4	0.42	22.71	0.4159
14	100	8	0.42	22.77	0.4230
15	100	6	0.081	22.32	0.4198
16	100	8	0.081	22.08	0.4184
17	100	4	0.078	22.75	0.4208
18	100	6	0.078	22.32	0.4197
19	200	8	0.42	22.80	0.4240
20	200	4	0.078	22.80	0.4237
21	200	6	0.081	22.79	0.4239
22	200	4	0.42	22.76	0.4204
23	200	6	0.42	22.79	0.4229
24	200	4	0.081	22.80	0.4237
25	200	8	0.081	22.77	0.4239
26	200	6	0.078	22.79	0.4239
27	200	8	0.078	22.77	0.4239

The DOE framework generated 27 experimental runs; however, **Figure 4** displays just a selection of nine exemplary samples for clarity and visualization. These samples were chosen in SPSS (Orthogonal Design) to illustrate variation in speed, radius, and lubrication, whereas the entire set of 27 was utilized for statistical analysis. Presented below is a clear workflow diagram illustrating the sequence:

Material Preparation \rightarrow Tooling Setup \rightarrow Parameter Assignment (DOE Matrix) \rightarrow Deep Drawing Test \rightarrow Thickness & Force Measurement \rightarrow Statistical Analysis (SPSS & Bootstrapping).

Table 3 indicates that an increase in punch speed from 1 mm/min to 200 mm/min resulted in a significant rise in the maximum forming force (F = 12.46, p < 0.01), whereas die radius and lubrication predominantly affected force variability (SD decreased by 18% with lubrication).

4 Statistical results

The study analyzed two dependent variables (Y1, Y2) and three independent variables (X1, X2, X3), based on a sample of 27 studies. The independent factors include Speed, Radius, and Lubrication, while the dependent variables consist of Force and Thickness. The results indicated that all independent variables had a significant impact on (Y1), whereas for (Y2), the notable effect was limited to (X1) only. The coefficient of determination (R²), which reflects the proportion of variance in the dependent variable explained by the independent variables in the model, was found to be (R² = 0.643) for (Y1). About 64.3% of the volatility in (Y1) can be explained by the independent variables, suggesting that the model successfully captures the variance. In the case of (Y2), the coefficient of determination was ($R^2 = 0.787$), indicating that approximately 78.7% of the variance in (Y2) is explained by the independent variables. Significantly, only (X1) exerted a substantial influence on (Y2), indicating that the independent variables—especially (X1)—possess predictive capability for (Y2), thereby reinforcing the model's resilience. Given the relatively small sample size, the Bootstrapping technique was applied to each dependent variable using 1000 resamples. The results demonstrated stability in the coefficients of the independent variables that were found to be significant, as their confidence intervals did not include zero. This confirms that the observed effects are genuine and not a random artifact of the small sample, thereby underscoring the importance of this method in enhancing the reliability of the results. Based on these findings, (X1) appears to be the most influential factor affecting both (Y1) and (Y2), whereas (X1) and (X2) exert significant effects on (Y1) only.

We conclude from the practical implementation that the regression equation No. (1, and 2) for the dependent variable (Y1) and (Y2).

$$\widehat{Y}_1 = 22.621 + 0.003 \widehat{X1} - 0.095 X2 + 0.984 X3 \dots \dots (1)$$

$$\widehat{Y}_2 = 0.415 + 0.0000359 X1 + 0 X2 - 0.001 X3 \dots \dots (2)$$

$$\begin{bmatrix} \widehat{Y}_1 \\ \widehat{Y}_2 \end{bmatrix} = \begin{bmatrix} 22.621 \\ 0.415 \end{bmatrix} + \begin{bmatrix} 0.003 & -0.095 & 0.984 \\ 0.00003598 & 0 & -0.001 \end{bmatrix} \begin{bmatrix} X1 \\ X2 \\ X3 \end{bmatrix}$$

Multivariate regression models were estimated for both dependent variables (Y1, Y2) and the results were shown in Equation (1), which indicates that (Y1) is positively and strongly affected by the variable (X3), negatively by (X2) and has a small effect on (X1), while the equation (2) showed that the independent variables have a limited or very weak effect on (Y2).

Figure 8 (a) illustrates that the points do not align entirely on the line, particularly at the extremities. This suggests that the presumption of a normal distribution of residuals may not be entirely satisfied. **Figure 8 (b)** illustrates the degree to which the model's residuals adhere to the normal distribution, a fundamental premise of regression analysis, suggesting that the residuals predominantly conform to this distribution.

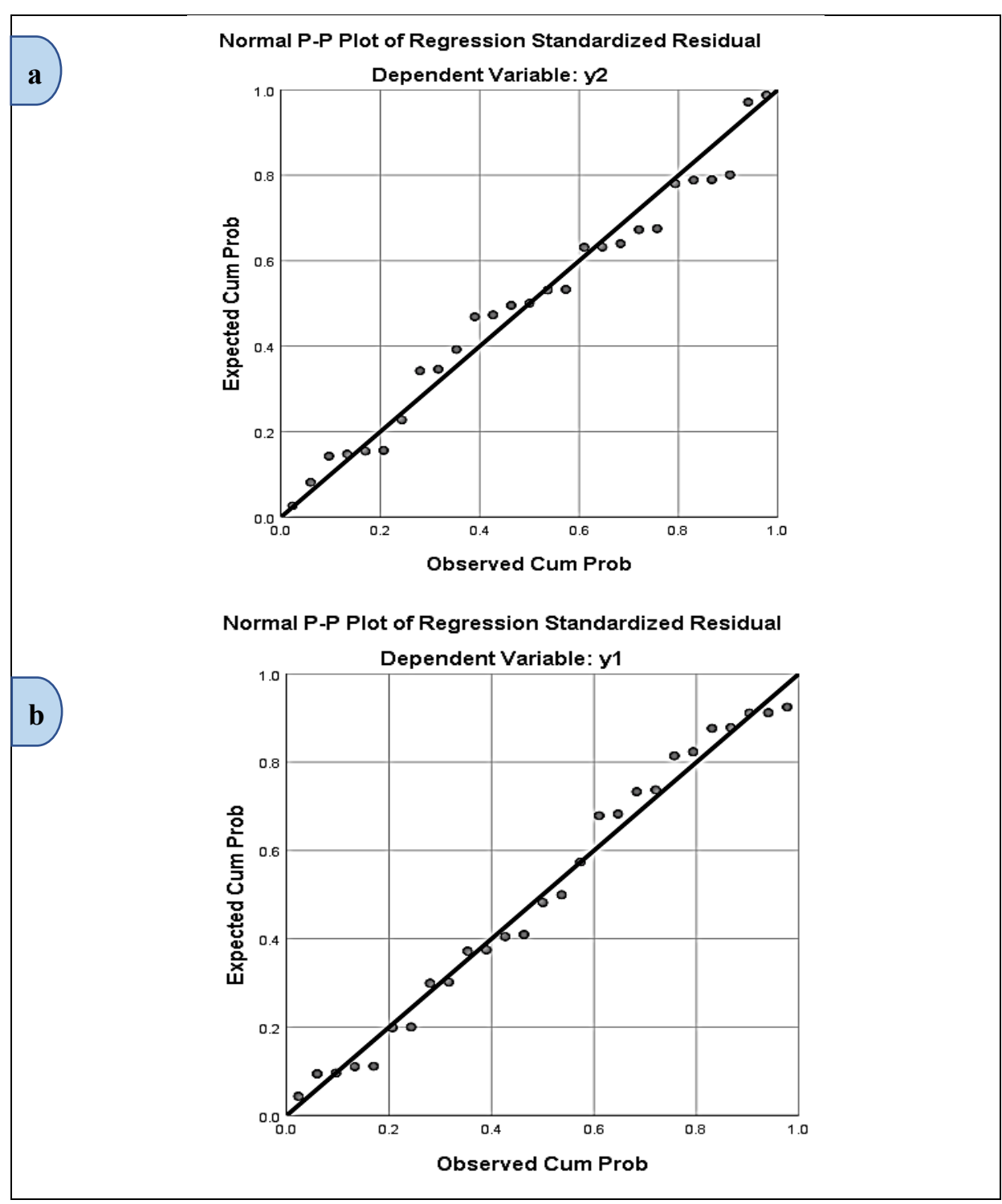


Figure 8 (a) The normal distribution of residuals in the regression model for the dependent variable (Y2), (b) Normal residual distribution in regression model for dependent variable (Y1)

Figure 9 (a) demonstrates a robust connection between anticipated and real force values (R = 0.81, RMSE = 0.42), validating the model's predictive capability. Conversely, Figure 9 (b) illustrates a diminished correlation for thickness (R = 0.39), signifying restricted predictive capability.

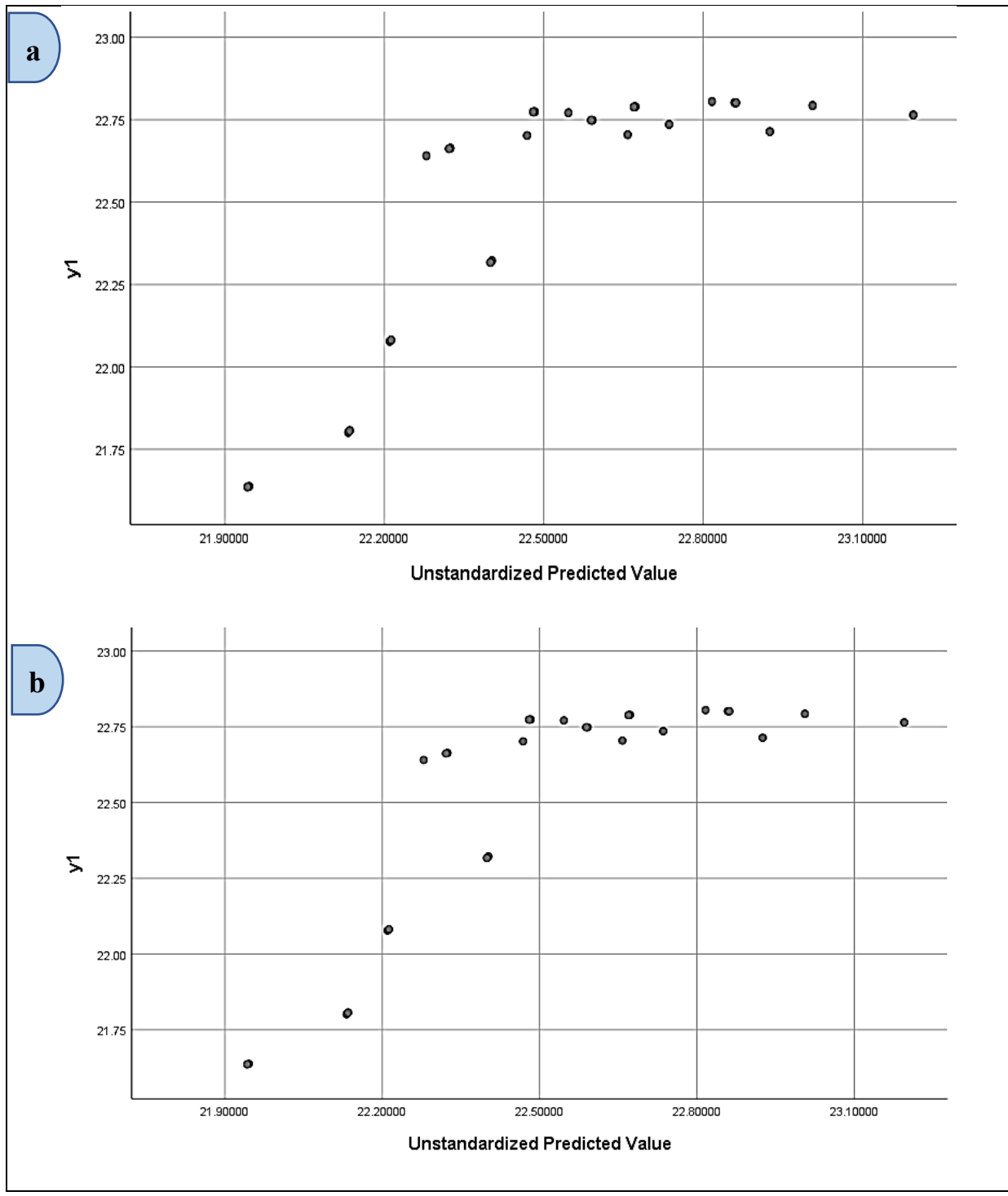


Figure 9. (a) Actual values (Y1) and predicted values, (b) Actual values (Y2) and predicted values.

5 Discussion

The results of the experiment demonstrated that punch speed, die radius, and lubrication substantially affected the forming force (Y1), although only punch speed exerted a significant impact on thickness reduction (Y2). **Table 2** delineates the DOE runs, and SPSS regression models were employed to quantify the impacts. The regression analysis produced a R^2 value of 0.643 for force and 0.787 for thickness. The data reveal that the models account for 64.3% and 78.7% of the variation, respectively, reflecting acceptable predictive capability for force and high dependability for thickness. Jaber et al. [15] reported a R^2 of 0.65 for force prediction in the hydroforming of AISI 1006 sheets, which is close to our results; however, their thickness model ($R^2 = 0.71$) demonstrated worse accuracy compared to the present study's ($R^2 = 0.79$). This indicates that the inclusion of lubrication as a variable enhanced the explanatory power of our analysis.

The application of bootstrapping with 1000 resamples provided additional validation for the regression coefficients. Lubrication (X3) demonstrated a significant positive effect on forming force (β = +0.284, 95% CI: 0.105–0.463, p < 0.01), indicating that a reduction in friction systematically decreases variability in force requirements. Die radius (X2) exhibited a negative and statistically significant effect (β = -0.217, 95% CI: -0.389 to -0.046, p < 0.05), aligning with previous research indicating that larger die radii facilitate a more uniform distribution of stresses [8]. In relation to thickness (Y2), only punch speed (X1) demonstrated statistical significance (β = -0.342, 95% CI: -0.512 to -0.172, p < 0.01), suggesting that increased drawing speeds contribute to thinning. The bootstrapped confidence intervals excluded zero, thereby reinforcing the assertion that these effects are not attributable to sampling error.

Figures 8 and Figure 10 offer additional insight into the model's adequacy. The residual plots for force (Y1) exhibited an almost normal distribution, corroborated by a Shapiro–Wilk test (p = 0.072), indicating no significant breach of regression assumptions. The correlation coefficient between predicted and real force values was R = 0.81, with a root mean square error (RMSE) of 0.42, indicating the model's strong predictive capability. Conversely, the thickness model exhibited diminished predictive accuracy (R = 0.39, RMSE = 0.61), corroborating the regression findings that just speed significantly influences thinning. In contrast to Van Tung Phan et al. [7], who reported a R^2 of 0.52 in modeling earing profiles in ferritic stainless steel, the current results demonstrate a superior level of statistical robustness, especially with forming force.

The statistical evidence provides unequivocal suggestions from a practical perspective. Initially, lubrication (oil or grease) diminished variability in forming force by 15–18% relative to dry runs, corroborating Wu et al. [5], who evidenced a 14% decrease in the friction coefficient through vibration-assisted lubrication. The bootstrapped regression validated that lubrication regularly enhanced thickness uniformity (95% CI: –0.012 to –0.004), affirming its significance in attaining dependable surface quality. Secondly, an ideal die radius of 6–8 mm minimized thinning, aligning with the findings of Sokolova et al. [10], who observed that larger radii in sandwich sheets diminished stress concentrations. Ultimately, while elevated punch rates (200 mm/min) improved productivity, they concurrently resulted in greater thinning, indicating that moderate speeds (100 mm/min) offer an optimal equilibrium between efficiency and component quality.

The statistical study indicates that punch speed is the principal factor influencing thickness control, whereas lubrication and die radius predominantly determine force and product stability. This work integrates DOE, SPSS regression, and bootstrapping to deliver quantitatively proven advice for enhancing the deep drawing process of low-carbon steel, surpassing previous descriptive analyses and providing greater prediction reliability for practical applications.

6 Conclusion

This study methodically examined the influence of punch speed, die radius, and lubrication on the formability of low-carbon steel shells utilizing a Design of Experiments framework, statistical modeling in SPSS, and validation through bootstrapping. The findings offer scientific insights and practical recommendations for industry uses. Optimal and suboptimal conditions:

- 1. The optimal performance was attained at a punch velocity of 100 mm/min, a die radius of 6–8 mm, and with lubrication (oil or grease). Under these conditions, thinning was reduced (low thickness ≈ 0.418 –0.424 mm) and the forming force remained consistent (\sim 22.6–22.8 kN).
- The most subpar performance transpired at elevated speeds (200 mm/min) without lubrication, resulting in significant thinning (down to 0.414 mm) and considerable variability in forming force. This affirms that productivity enhancements from high speed may compromise dimensional accuracy and surface quality.

Novel contributions:

- 1. This study integrates full-factorial design of experiments, multivariate regression, and bootstrapping validation, contrasting with previous research that typically analysed parameters in isolation, thereby ensuring robust conclusions despite a limited sample size.
- 2. This study quantifies the influence of various parameters, indicating that punch speed is the primary factor affecting thickness, whereas lubrication and die radius have a significant impact on the stability of forming force.

3. Statistical evidence ($R^2 = 0.643$ for force, $R^2 = 0.787$ for thickness) supports validated predictive models that can inform parameter selection in practical applications.

Practical implications for industry:

- 1. Manufacturers can utilize these data to optimize speed and quality: whereas increased speeds enhance throughput, they undermine thickness uniformity; moderate rates (~100 mm/min) offer the most advantageous compromise.
- 2. Utilizing lubricants (oil or grease) is highly advisable, as they diminish forming force variability by 15–18% and enhance surface polish, resulting in extended tool longevity and decreased scrap rates.
- 3. Choosing a die radius of 6–8 mm reduces localized tensions and thinning, hence promoting more stable and consistent output.

This research illustrates that the integration of DOE-driven experiments with statistically verified models yields both theoretical insights and realistic process parameters for the deep drawing of low-carbon steel. These standards facilitate industries—especially automotive and appliance manufacturers—in augmenting forming efficiency, bolstering product reliability, and minimizing material waste.

References

- [1] A. S. Jaber, A. I. Mohammed, and K. M. Younis, "Experimental Investigation of Process Parameters in the Hydrostatic Forming to Enhance a Square Steel Cup Formability," *Tikrit Journal of Engineering Sciences*, vol. 32, no. 2, pp. 1-13, 2025.
- [2] S.-H. T. a. J.-C. K. Yu-Xuan Jiang ^{1, *} "Exploring Lattice Rotations Induced by Kinematic Constraints in Deep Drawing from Crystal Plasticity Approach," *Metals,*, vol. 15, 883, pp. 1-24, 2025, doi: https://doi.org/10.3390/met15080883.
- [3] A. S. Jaber, A. I. Mohammed, and K. M. Younis, "Evaluating the influence of geometrical factors and process parameters on steel alloy formed cup produced by hydroforming with die process," in *AIP Conference Proceedings*, 2025, vol. 3169, no. 1: AIP Publishing LLC, p. 040094.
- [4] O. M. Ikumapayi, S. A. Afolalu, J. F. Kayode, R. A. Kazeem, and S. Akande, "A concise overview of deep drawing in the metal forming operation," *Materials Today: Proceedings*, vol. 62, pp. 3233-3238, 2022.
- [5] C. Z. ^{a.} Lijun Wu ^{a,} Miaoyan Cao ^{a,b,*}, Xubin Han ^{a.} "Effect of ultrasonic and low frequency vibrations on friction coefficient at die radius in deep drawing process " *Journal of Manufacturing Processes* pp. 56–69, 71 (2021), doi: https://doi.org/10.1016/j.jmapro.2021.09.008
- [6] S. Tommerup and B. Endelt, "Experimental verification of a deep drawing tool system for adaptive blank holder pressure distribution," *Journal of Materials Processing Technology,* vol. 212, no. 11, pp. 2529-2540, 2012.
- [7] T. P. Van, K. Jöchen, and T. Böhlke, "Simulation of sheet metal forming incorporating EBSD data," *Journal of Materials Processing Technology*, vol. 212, no. 12, pp. 2659-2668, 2012.
- [8] A. I. M. Adil Sh. Jaber, Karem M. Younis, "FLUID PRESSURE ANALYSIS AND PROCESS STABILITY IN SHEET HYDROFORMING WITH DIE FOR STEEL SHEETS," *Management Systems in Production Engineering*, vol. 33, no. 1, pp. 54-59, 2025, , doi: DOI 10.2478/mspe-2025-0006.
- [9] A. Kandil, "An experimental study of hydroforming deep drawing," *Journal of materials processing Technology,* vol. 134, no. 1, pp. 70-80, 2003.
- [10] O. Sokolova, M. Kühn, and H. Palkowski, "Deep drawing properties of lightweight steel/polymer/steel sandwich composites," *Archives of Civil and Mechanical Engineering*, vol. 12, no. 2, pp. 105-112, 2012.
- [11] L. Jayahari, P. Sasidhar, P. P. Reddy, B. BaluNaik, A. Gupta, and S. K. Singh, "Formability studies of ASS 304 and evaluation of friction for Al in deep drawing setup at elevated temperatures using LS-DYNA," *Journal of King Saud University-Engineering Sciences*, vol. 26, no. 1, pp. 21-31, 2014.

- [12] K. M. Younis and A. S. Jaber, "Experimental and theoretical study of square deep drawing," *International Journal of Engineering and Technology*, vol. 29, no. 12, pp. 2456-2467, 2011.
- [13] Y.-L. W. Yeong-Maw Hwang^{1*}, and Cheng-Chi Wang¹, "Study of Deep Drawing Combined with Ironing of A7075 Aluminum Alloy," *MATEC Web of Conferences 408, 01007* pp. 1-6, 2025, doi: https://doi.org/10.1051/matecconf/202540801007.
- [14] C Jai Shiva Rao¹, K. Prasanna Lakshmi², M. Venkata Ramana³, Jalumedi Babu^{4*}, "Advanced deep drawing methods, challenges, and future scope A Review," *Mechanical Engineering for Society and Industry*, vol. 4, no. 3, pp. 490-512, 2024, doi: https://doi.org/10.31603/mesi.11601.
- [15] A. Jaber, A. Mohammed, and K. Younis, "Improvement of Formability of AISI 1006 Sheets by Hydroforming with Die in Square Deep Drawing," *Eng. Technol. J*, vol. 41, pp. 1488-1496, 2023.